Electronic Supplementary Material (ESI) for Catalysis Science & Technology.

Supporting Information

Methane Activation over Boron Nitride Catalyst Driven by In Situ Formed Molecular Water

Yang Wang,[a] Li-Yang Zhao,[b] Lei Shi,[a] Jian Sheng,[a] Wei-Ping Zhang,[a]

Xiao-Ming Cao,*[b] Pei-Jun Hu,[b] and An-Hui Lu*[a]

a. State Key Laboratory of Fine Chemicals,

School of Chemical Engineering,

Dalian University of Technology, Dalian 116024, P. R. China.

E-mail: anhuilu@dlut.edu.cn

b. Centre for Computational Chemistry and Research Institute of Industrial Catalysis, School of Chemistry and Molecular Engineering,

East China University of Science and Technology, Shanghai 200237, P. R. China.

E-mail: xmcao@ecust.edu.cn

1. Experimental Section

Catalyst preparation

All catalytic testing was done using hexagonal boron nitride (Aladdin). Before using, sodium ions were leached out with a reflux in 3 mol L^{-1} ammonia at 80 °C for 6 times, followed extensive washing with ultrapure water (40 times, 50 mL water each).

Catalytic tests

Catalytic reactions were carried out in a packed-bed quartz microreactor (I.D.= 8 mm). The reaction mixture was $CH_4/O_2/N_2$ with a molar ratio of 2/1/4 at atmospheric pressure. Flow rate was fixed at 35 mL min^{-1}, and reaction temperature was varied in the range of 640-740 °C. Reactants and products were analyzed by an online gas chromatograph (Techcomp, GC 7900). A Porapak Q 2 and molecular sieve 5A column, connected to a TCD were used to analyze the O_2, N_2, CH_4, H_2, CO, C_2H_4, C_2H_6, and CO_2. Conversion was defined as the number of moles of carbon converted divided by the number of moles of carbon present in the feed. Selectivity towards CO, C_2H_4, C_2H_6, and CO_2 was defined as the number of moles of carbon in the product divided by the number of moles of carbon reacted. Selectivity towards H_2 was defined as the number of moles of hydrogen in the H_2 divided by the number of moles of hydrogen reacted. The carbon balance was checked by comparing the number of moles of carbon in the outlet stream to the number of moles of carbon in the feed. Under our typical evaluating conditions, the carbon balance was within ±2%. N_2 was used as the internal standard to account for the volume expansion in the reaction.

Catalyst characterization

X-ray powder diffraction (XRD) measurements were operated on a PANalytical X'Pert3 Powder diffractometer using Cu Kα radiation (λ = 0.15406 nm). The tube voltage was 40 kV, and the current was 40 mA.

Transmission electron microscopy (TEM) images were recorded on a FEI

TECNAI F30 microscope, operating at an accelerating voltage of 300 kV.

X-ray photoelectron spectroscopy (XPS) analysis was performed on an Omicron Sphera II hemispherical electron energy analyzer with an in-situ reaction cell attached to the instrument. Monochromatic Al K X-ray source (1486.6 eV, anode operating at 15 kV and 300 W) was used as incident radiation. The binding energy of the element was calibrated using an C 1s photoelectron peak at 284.5 eV. Before the measurements, all the samples were treated in-situ at 500 °C for 1 hour under an Ar stream (32 mL min^{-1}) and then moved to the measured chamber under vacuum conditions.

Nitrogen adsorption-desorption isotherms were measured with a Micromeritics TriStar 3000 adsorption analyzer. Before the measurements, the sample was degassed at 200 °C for 4 hours. The specific surface area was calculated from the adsorption data in the relative pressure range from 0.05 to 0.3 using the Brunauer-Emmett-Teller (BET) method.

Solid-state magic-angle-spinning nuclear magnetic resonance (MAS NMR) spectra were recorded on an Agilent DD2-500 MHz spectrometer. ^{1}H MAS NMR experiments were carried out at 499.8 MHz, using a 4-mm MAS NMR probe with a spinning rate of 10 kHz. ^{1}H MAS NMR spectra were accumulated for 32 scans with a 5 second recycle delay. The chemical shifts were referenced to tetramethylsilane (TMS). Prior to testing, the sample was dehydrated at 400 °C for 1 h at 10^{-4} Pa and then transferred to a 4-mm MAS rotor in a home-made device without exposure to air.

The amount of coke deposited was determined by combustion of the deposited material on a thermogravimetric (TG) analyzer STA 449 F3 (NETZSCH). The sample was exposed to a mixture of 20% O_2 in N_2 flowing at 40 mL/min and oxidized from ambient temperature to 950 °C at a heating rate of 5 °C/min. The CO_2 generated was monitored by on-line mass spectrometry (MS, Pfeiffer, OminStar^{TM}). The amount of deposited coke was calculated from the weight loss of the samples.

In-situ infrared spectroscopy

In-situ Fourier transform infrared spectra (FT-IR) were recorded under reaction conditions on a Nicolet 6700 FT-IR spectrometer equipped with mercury cadmium telluride (MCT) detector. The BN catalyst of ~30 mg was compressed as a thin disk (Φ = 1.2 cm), and placed in a quartz transmission cell equipped with CaF_2 windows and a thermocouple mount that allowed direct measurement of the surface temperature. Spectra were averaged over 64 scans in the range 400-4000 cm^{-1} with a 4 cm^{-1} resolution. Prior to collecting spectra, catalysts were pretreated for 1 hour at 550 °C in helium (40 mL min^{-1}). The gas composition at the reactor outlet during *in-situ* FT-IR experiments was controlled by online mass spectrometry (MS, Pfeiffer, OminStar™). The following mass-to-charge (m/z) signals were analyzed: 2 (H_2), 16 (CH_4), 18 (H_2O), 28 (C_2H_6, C_2H_4, CO) and 44 (CO_2).

Isotope-labelling experiments

Isotopic tracer experiments were performed in a packed bed single pass flow microreactor. The chemical and isotopic compositions of the reactor effluent were measured by online mass spectrometry (MS, Pfeiffer, OminStar™). In the deuterium-labelling studies, the *h*-BN catalyst was initially treated at 590 °C under N_2 (40 mL min^{-1}) for 1 hour, and then a 15-hour H/D exchange process on the BN surface was accomplished by passing a He feed (40 mL min^{-1}) through a water saturator thermostatted at 25 °C. Heavy water (D_2O, Cambridge Isotope Lab., 99.9%) was not further purified. Subsequently, the deuterated BN catalyst was purged with the dry N_2 (40 mL min^{-1}) for 3 hours to remove the excess D_2O. CH_4, O_2 or a mixture of the two was then directly pulsed into the deuterated BN catalyst using N_2 (20 mL min^{-1}) as the carrier gas. The products were analyzed by a mass spectrometer with the following mass-to-charge (m/z) signals: 15 for CH_4, 32 for O_2, 18 for H_2O, 19 for HDO and 20 for D_2O.

Density functional theory calculation

The surface reaction processes occurring at the zig-zag edge of oxidized *h*-BN and BNOH were modeled based on the periodic spin-polarized density

functional theory calculations utilizing the generalized gradient approximation (GGA) exchange-correlation functional of Perdew-Burke-Ernzerhof (PBE) form implemented in VASP package. The Grimme's empirical three-body dispersion correction in the scheme of Becke–Johnson dampling was also included for all the calculations to accurately describe van der Waals interaction. The electron-ion interactions were modelled utilizing the projector augmented wave (PAW) pseudopotential and the plane wave basis-set was expanded to the converged cut-off energy of 500 eV. The exposed $(10\bar{1}0)$ facet observed at the TEM image was selected to model the zigzag edge of the single-layer *h*-BN utilizing a 10.032 Å ×10.000 Å × 20.031Å, *p* (4×1) slab with 5 B-N layers along the Z direction. The corresponding Brillouin integration for the unit cell was sampled using 3 × 1 × 1 Monkhorst-Pack grid. All the stationary points for gaseous reactions were optimized at M06-2x/aug-cc-pvTZ level utilizing Gaussian 09 package. The subsequent vibrational frequency analysis was also performed to identify them either as minima or as the first-order saddle points corresponding to transition states followed by the intrinsic reaction coordinate (IRC) calculations to verify that each transition state is located at the reaction pathway connecting two minima. The adsorption energy E_{ad} was defined as follows:

$$E_{ad} = E_{sur} + E_x - E_{x^*}$$

where E_{sur}, E_x and E_{x^*} respectively denote the total energies of bare surface, gaseous species, and the corresponding surface species. The positive value of E_{ad} suggests that the species can adsorb over the surface. The greater E_{ad} is, the more strongly the specie x binds with the surface. The asterisk denotes the surface species.

2. Figures and tables described in the main text and supplementary information

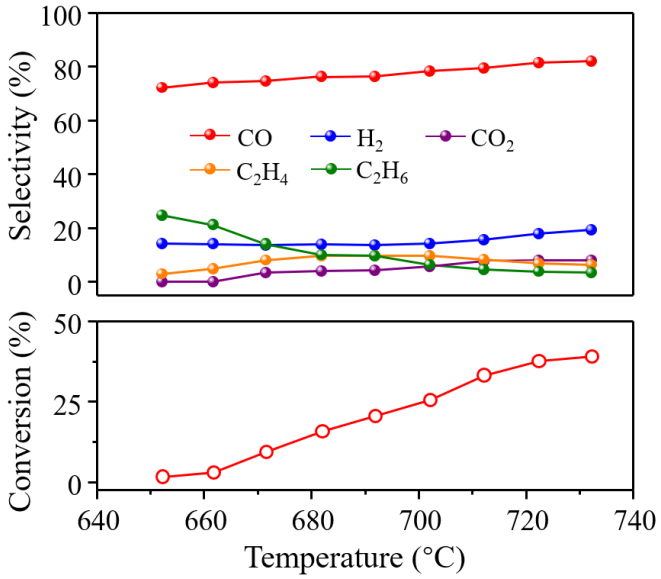

Fig. S1 Influence of temperature on the methane conversion and products selectivity over the *h*-BN catalyst. Reaction conditions: catalyst, 100 mg; gas feed, 28.6 vol% CH_4, 14.3 vol% O_2, and N_2 balance; Gaseous hourly space velocity 21,000 mL g_{cat}^{-1} h^{-1}.

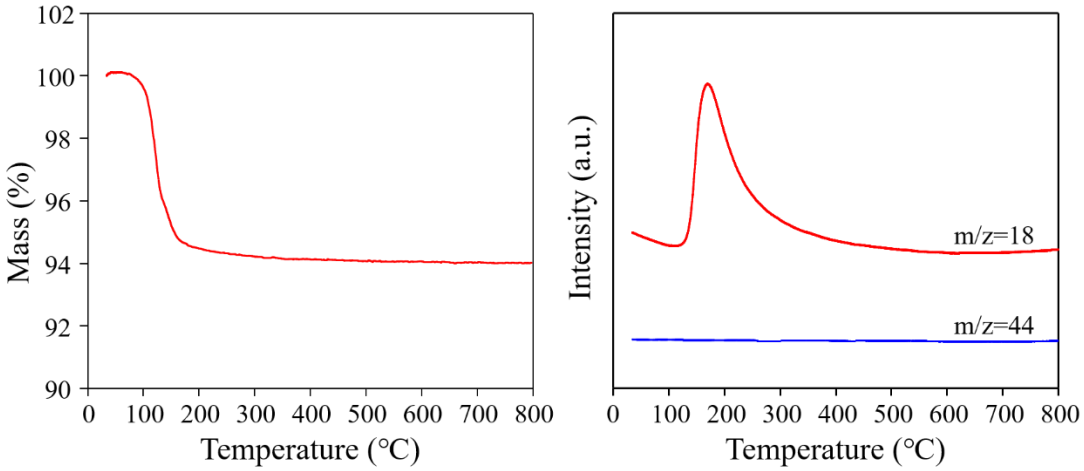

Fig. S2 Thermogravimetry (TG)-MS profiles under a TPO environment of *h*-BN catalyst after 20-h test.

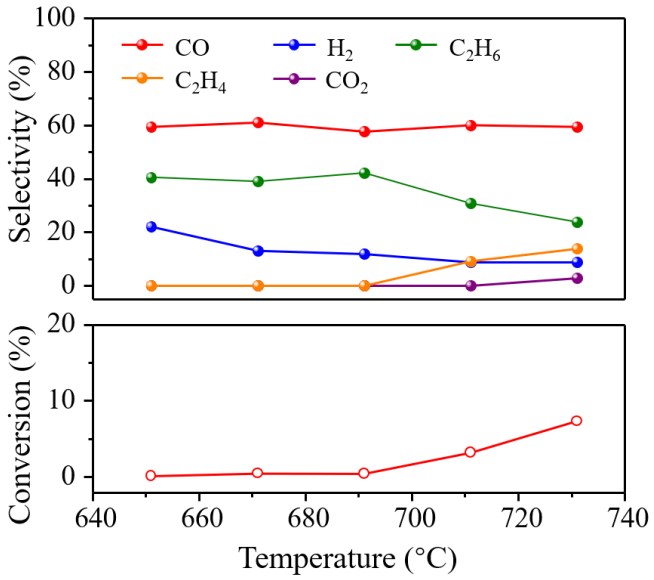

Fig. S3 Influence of temperature on the catalytic activity and selectivity in oxidation of methane over the quartz sand. Reaction conditions: catalyst, 100 mg; gas feed, 28.6 vol% CH_4, 14.3 vol% O_2, and N_2 balance; Gaseous hourly space velocity 21,000 mL g_{cat}^{-1} h^{-1}.

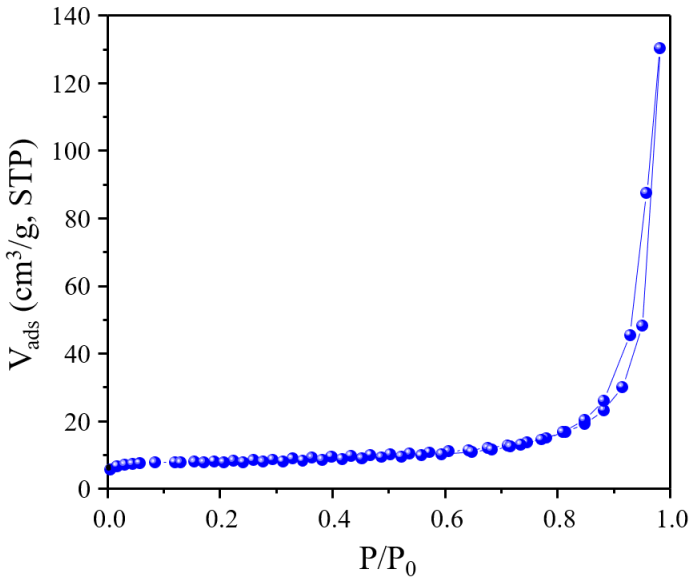

Fig. S4 N_2 sorption isotherm of *h*-BN.

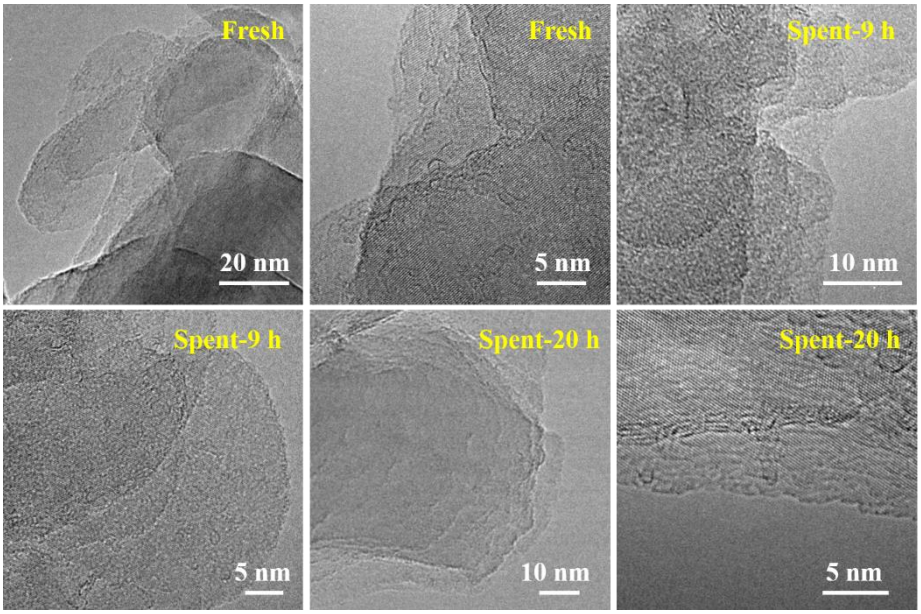

Fig. S5 High-resolution TEM images of the fresh and spent *h*-BN catalyst after a 20-h test.

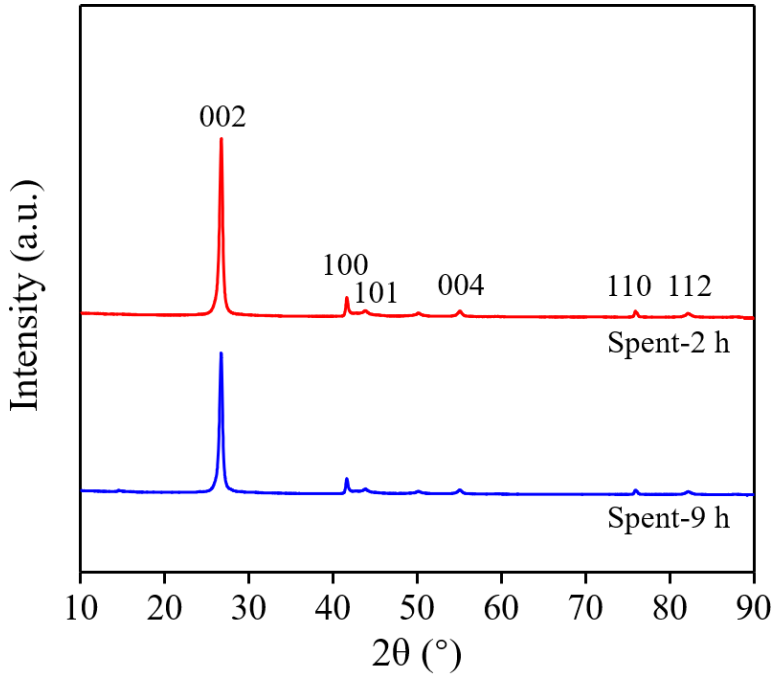

Fig. S6 XRD patterns of *h*-BN catalyst after 2-h and 9-h test.

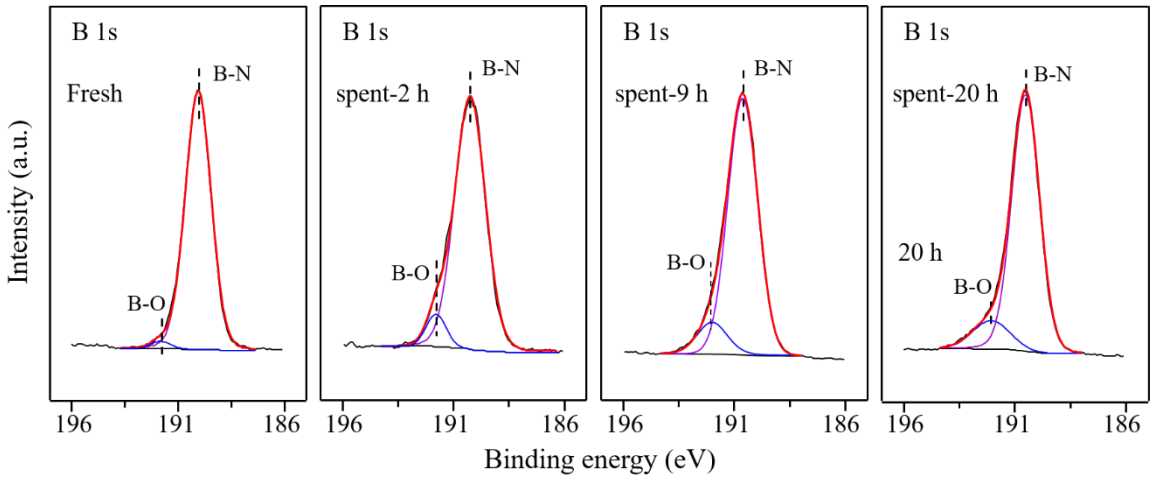

Fig. S7 B 1*s* XPS spectra of the fresh catalyst and spent catalyst after 2-h, 9-h and 20-h test.

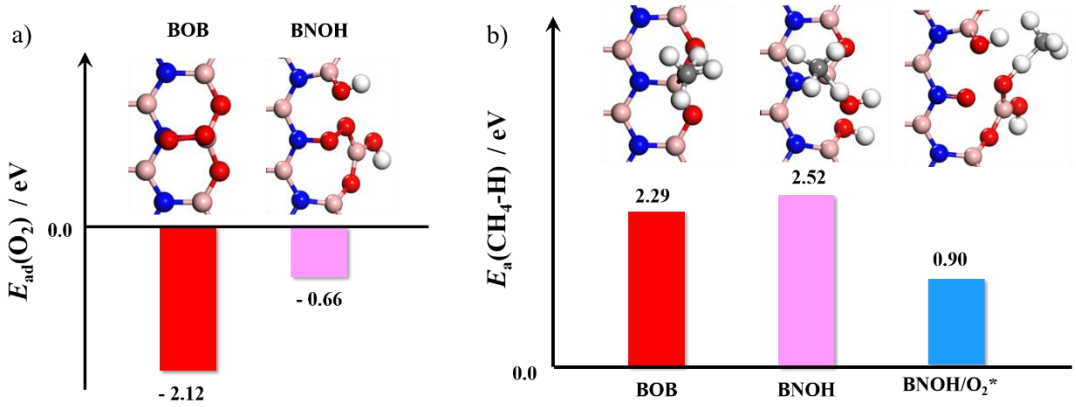

Fig. S8 (a) The chemisorption energy of O_2; (b) The energy barrier of the first C-H bond scission of CH_4.

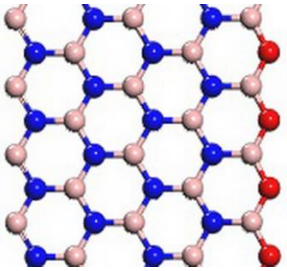

Fig. S9 The geometry structure of oxidized *h*-BN.

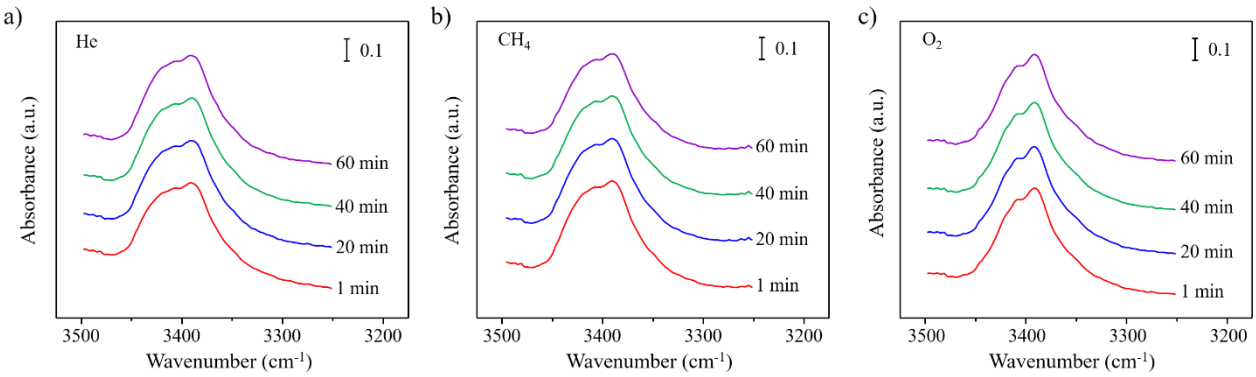

Fig. S10 FT-IR spectra of B-OH vibration over the *h*-BN catalyst under a) He, b) CH_4, and c) O_2 atmospheres.

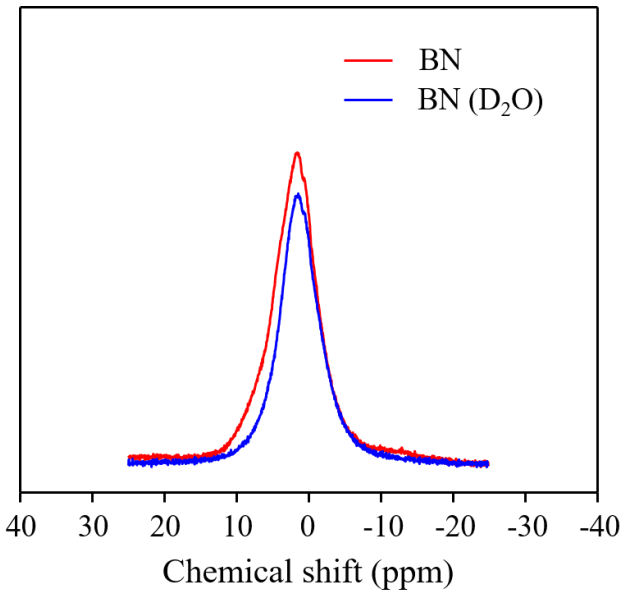

Fig. S11 ^{1}H NMR spectra of *h*-BN catalyst before and after D_2O exchanged process.

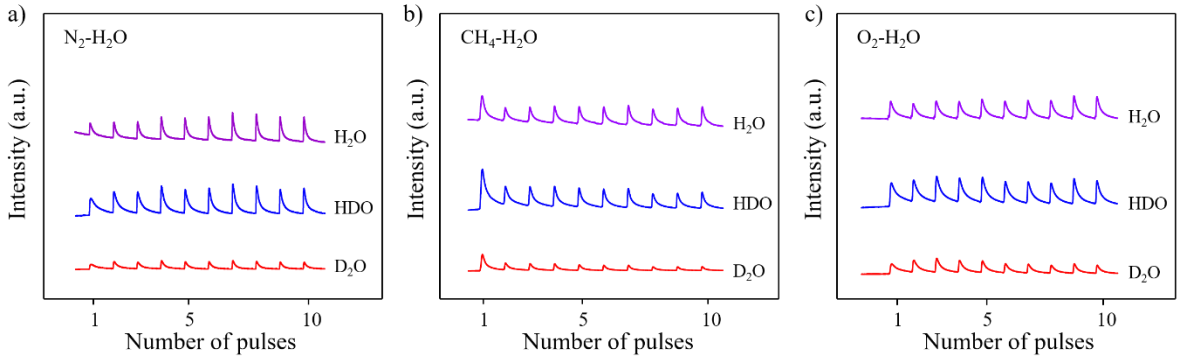

Fig. S12 Mass spectra of H_2O, HDO and D_2O species upon pulsing a mixture of a) N_2 and H_2O; b) CH_4 and H_2O; c) O_2 and H_2O onto the deuterated *h*-BN catalyst.

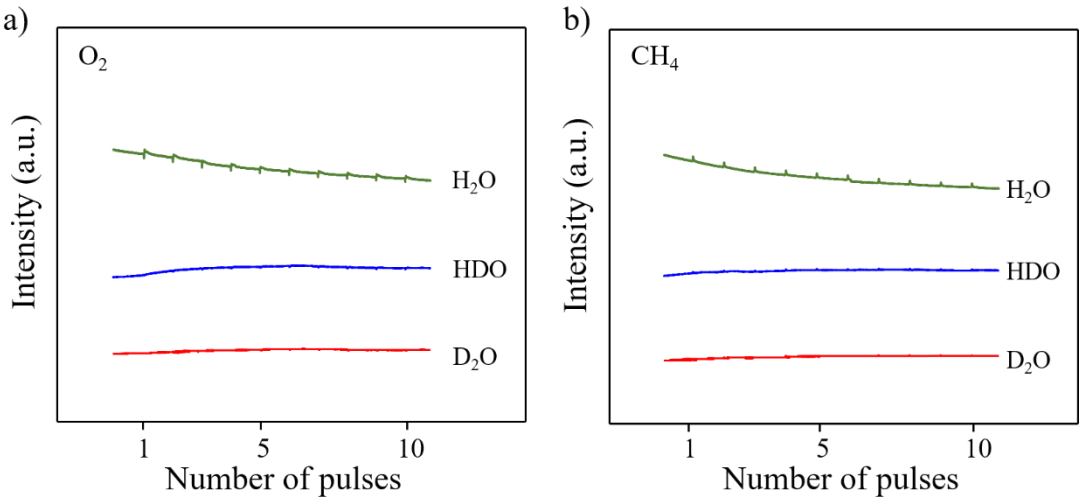

Fig. S13 Mass spectra of H_2O, HDO and D_2O species upon pulsing a) O_2; b) CH_4 onto the deuterated *h*-BN catalyst.

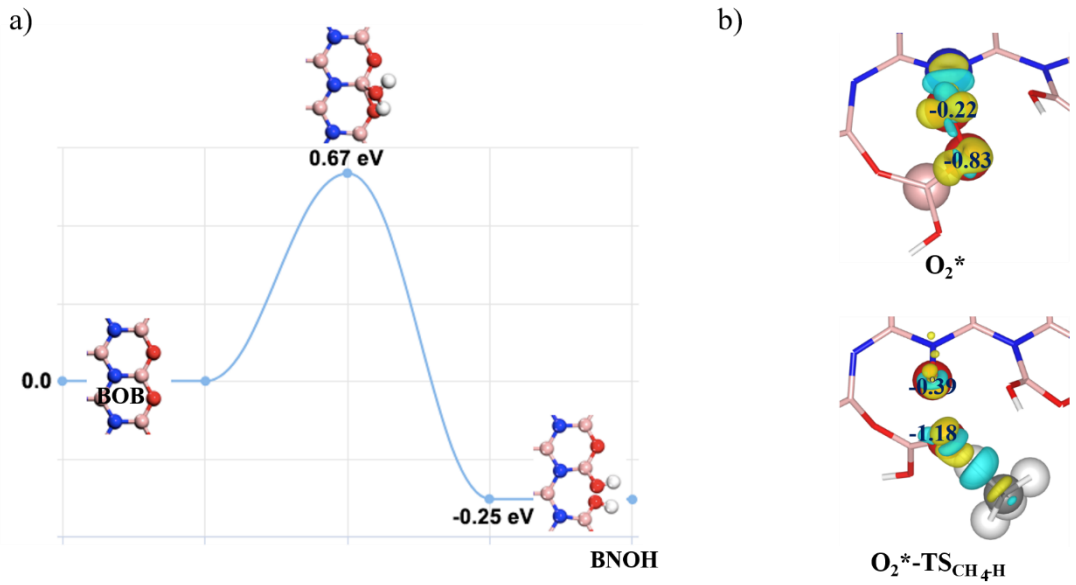

Fig. S14 (a) The energy profile of the transformation of oxidized *h*-BN to BNOH; (b) The bader charges and difference charge density of O_2^* respectively during its adsorption on BNOH and the first CH_4 oxidative dehydrogenation.

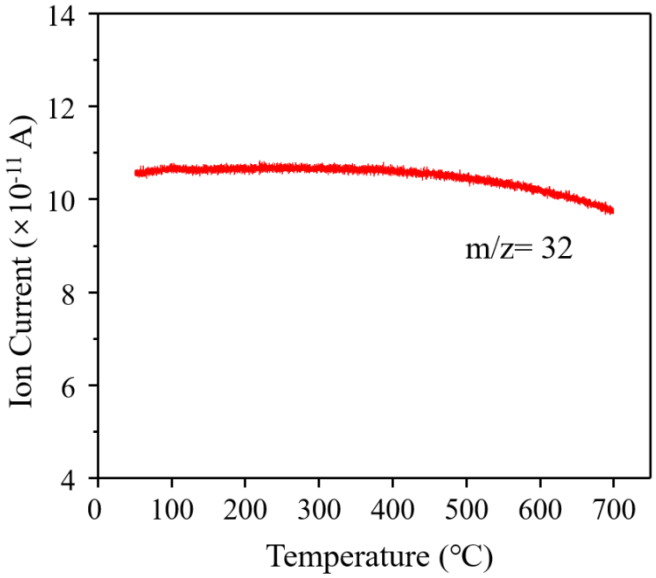

Fig. S15 O_2 TPD-MS profile over *h*-BN catalyst.

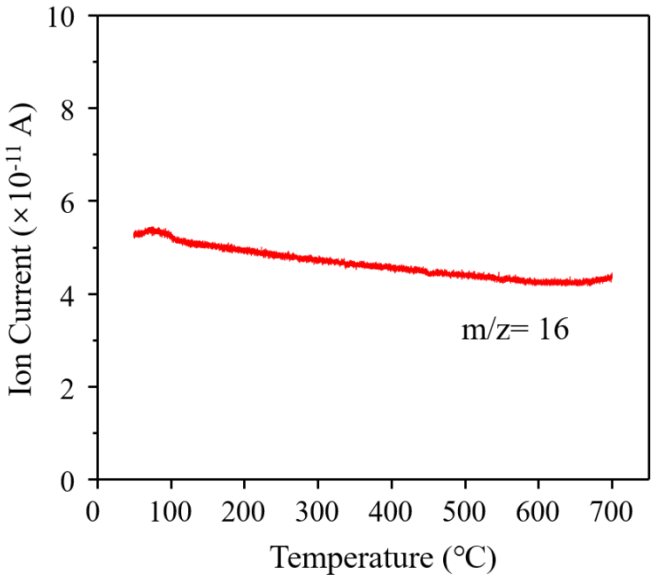

Fig. S16 CH_4 TPD-MS profile over *h*-BN catalyst.

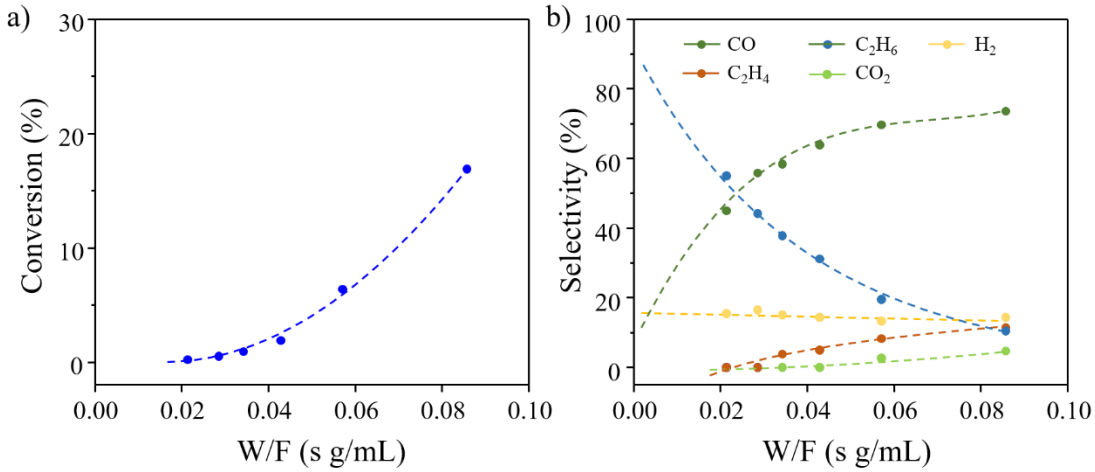

Fig. S17 Dependence of a) methane conversion and b) products selectivity on W/F over *h*-BN catalyst. Reaction conditions: GHSV =42000-168000 $mLg^{-1}h^{-1}$, $CH_4/O_2/N_2$= 2/1/4, 690 °C.

Table S1. Free energies variation (ΔG) and free energy barriers (G_a) of possible elementary steps occurring in the gas phase

Steps	Reaction pathways	ΔG / eV	G_a / eV
1	$CH_3O\bullet \rightarrow HCHO + H\bullet$	0.02	1.16
2	$CH_3O\bullet + O_2 \rightarrow HCHO + OOH\bullet$	-1.10	2.91
3	$HCHO + CH_3\bullet \rightarrow CHO\bullet + CH_4$	-0.64	1.56
4	$CHO\bullet + O_2 \rightarrow CO + OOH\bullet$	-1.37	0.78
5	$CHO\bullet \rightarrow CO + H\bullet$	-0.26	0.69
6	$CH_3\bullet + CH_3\bullet \rightarrow C_2H_6$	-2.06	
7	$H\bullet + H\bullet \rightarrow H_2$	-3.41	
8	$H\bullet + CH_4 \rightarrow CH_3\bullet + H_2$	-0.18	1.49
9	$H\bullet + C_2H_6 \rightarrow C_2H_5\bullet + H_2$	-0.45	1.35
10	$O_2 + H\bullet \rightarrow OOH\bullet$	-1.12	0.97
11	$CH_3\bullet + OOH\bullet \rightarrow CH_3OOH$	-1.28	
12	$CH_3OOH \rightarrow CH_3O\bullet + OH\bullet$	0.32	0.32
13	$OH\bullet + H\bullet \rightarrow H_2O$	-4.04	
14	$C_2H_6 + CH_3\bullet \rightarrow C_2H_5\bullet + CH_4$	-0.27	1.79
15	$C_2H_5\bullet \rightarrow C_2H_4 + H\bullet$	0.68	